AHMED A. ELASHIRY
Beni-Suef University, Beni-Suef, Egypt

MOHAMED A. YOUSSEF
Assiut University, Assiut, Egypt

MOHAMED A. ABDEL HAMID
Beni-Suef University, Beni-Suef, Egypt

PHASE-PHASE AND PHASE-CODE METHODS MODIFICATION FOR PRECISE DETECTING AND PREDICTING THE GPS CYCLE SLIP ERROR

ABSTRACT

There are three well-established detecting methods for cycle slip error, which are: Doppler measurement method, Phase-Code differencing method, and Phase-Phase Differencing Method. The first method depends on the comparison between observables and the fact that Doppler measurements are immune to cycle slip error. This method is considered as the most precise method for cycle slip detecting, because it succeed in detecting and predicting the smallest cycle slip size (1 cycle) in case the local oscillator has low bias. The second method depends on the comparison between observables (phase and code) and the code measurements are immune to the cycle slip error. But this method can't detect or predict cycle slip size smaller than 10 cycles, because the code measurements have high noise. The third method depends on the comparison between observables (phase 1 and phase 2) and the phases measurements that have low noise. But this method can't detect or predict cycle slip size smaller than 5 cycles, because the ionospheric change might have a high variation.

For enhancing the precision of the last two methods in detecting the smallest cycle slip which size reaches 1 cycle, a new algorithm was developed in this research to determine the change in the ionospheric values and the code bias from epoch to epoch. That is done by solving all observables equations by least square technique. This modification on these methods succeed in detecting and predicting cycle slips of size of 1 cycle.

Keywords:
GPS, Cycle slip, Phase-Code differencing, Phase-Phase differencing, Doppler measurements.

INTRODUCTION

Global Positioning System (GPS) is a satellite based navigation and surveying system for determining the precise position and time, using radio signals from the satellites, in real-time or post-processing mode [Ren et al. 2011]. It consists of a constellation of 32 satellites in six different orbits which give the information of the position of the GPS receiver user. If there are four or more GPS satellites in unobstructed line of sight with the receiver, the precise spatial co-ordinates can be obtained [Dawod, 1991]. Each GPS satellite transmits two carrier phase: L1 = 1575.42 MHz; and L2 = 1227.60 MHz modulated with two types of codes and a navigation message. The L1 signal is modulated with a precise (P) code, known also as the Precise Positioning Service (PPS), and a coarse acquisition (C/A) code, which is known also as the Standard Positioning Service (SPS); the L2 signal is modulated with P code only [Dawod, 1991; Raju, 2004]. This means the GPS carrier phase observations quality play an important role in high precision GPS static or kinematic positioning. However, due to internal tracking problems of GPS receiver or signal interruption of the antenna from the satellite, the continuous original carrier phase observations are destroyed, generating cycle slips and gross errors [Wu et al. 2010]. The main causes of the cycle-slip are listed below [Kim, 2012]:

1. Obstructions of the satellite signal due to trees, buildings, bridges, mountains, etc.
2. Low signal-to-noise ratio (SNR) or alternatively carrier-to-noise-power-density ratio (C/N0) due to bad ionospheric conditions, multipath, high receiver dynamics, or low satellite elevation angle.
3. Failure in the receiver software which leads to incorrect signal processing.

The cycle slip is a sudden jump in the phase observations as shown in Figure 1 [Goad, 1985], and it may be as small as one or a few cycles, or contain millions of cycles, which directly affect the GPS positioning precision. Therefore, the precise detecting and predicting for the gross errors and cycle slips is an important pre-processing step in high precision GPS carrier phase positioning and applications [Wu et al. 2010; Goad, 1985].
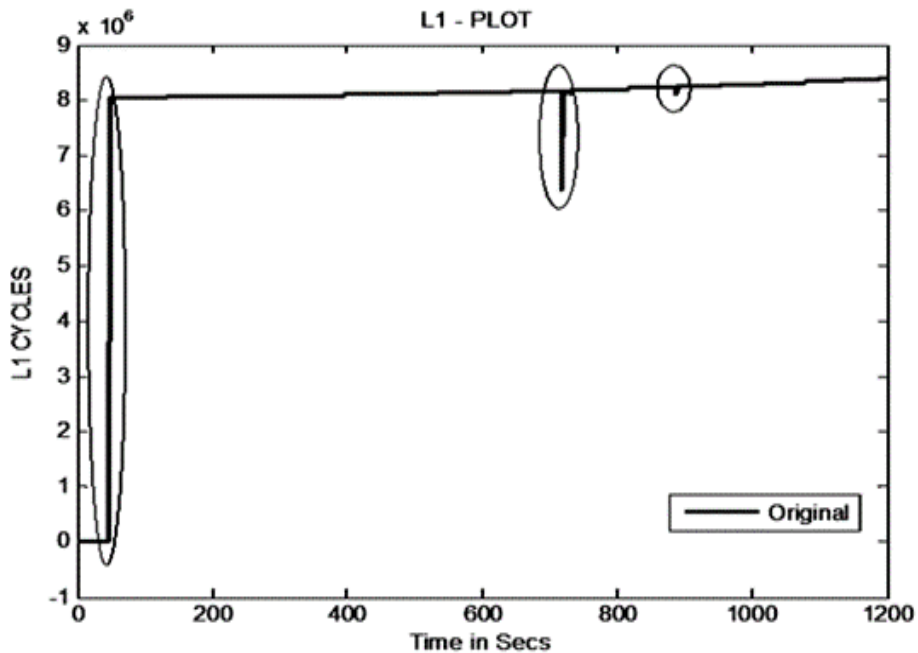
Fig. 1. Examples of cycle slips in observable data (L1) [source: Goad, 1985]

OBSERVATIONS DATA

Many cycle-slip detection methods have been proposed since the early 1980s [Goad, 1985] established the first cycle slip predicting method based on ionospheric residual (PIR). Bastos et al. studied Kalman filtering technique for filtering observables data from cycle slip to improve the positioning accuracy [Wu et al., 2010]. Also Kleusberg et al. established a new approach for cycle slip predicting based on high-order differencing concept [Seeber, 2003]. Recently, several new methods have been proposed for cycle slip detection based on comparisons between the GPS measurements, based on high-order differencing concept, where [Dai, 2012] studied all GPS measurements (phases and codes) and the estimated Doppler shift in the RINEX observations file and concluded that the Doppler measurement method is the most precise one. From his study, many detected methods were established which are; Phase-Code differencing method, Phase-Phase Differencing Method and Doppler measurement method.

Later [Cai et al., 2013] was developed a new approach for cycle slip detecting and repairing under high ionospheric activity using undifferenced dual--frequency GPS carrier phase observations with new algorithms. These algorithms integration was allowed uniquely detecting and determining for the cycle slips (≥ 5 cycles), even under high ionospheric activities, and Banville et al. [Banville et al., 2012] studied the decoupled-clock model to improve cycle-slip correction capabilities and use it in single frequency point precise positioning (PPP) to improve the positioning results. Implemented Doppler-aided cycle slip detecting and repairing method, using a simplified oscillator model with some modification to avoid the influence of the local oscillator bias was proposed by Ren et al. [Ren et al., 2011] which lead to high precision in predicting and repairing the cycle slips at real time kinematics positioning method for size equal 1 cycle.

Another solution was developed by Liu [Liu, 2010] with a new automated cycle slip detection and repair method that is based on only one single dual-frequency GPS receiver. This method used the ionospheric total electron contents (TEC) rate (TECR) and Melbourne-Wübbena wide lane (MWWL) linear combination to uniquely determine any cycle slip even under very high level of ionospheric activities and on both L1 and L2 frequencies. In [Wu et al., 2010] a new approach depended on using three groups of uncorrelated dual-frequency observation was established. This approach helped on repairing and detecting various real-time cycle slips and gross error under the long sampling condition.

Zhang and Li in the cycle of publications [Zhang and Li, 2012; Li et al., 2013; Li et al., 2014] has propose method for rapid ambiguity fixing in PPP to avoid a long re-initialization time. In these method the predicted atmospheric delays is use to correct the observations which suffer from signal interruptions, so real-time PPP with integer ambiguity fixing becomes more feasible in practice.

The observational data which processed in this research was taken from master thesis work for a demonstrator in Mining and Metallurgy Department in Assiut University. The collected data was for two fixed points called (C and R) at two different places in Assiut city in Egypt (Fig. 2). They were observed by GPS receiver (ASHTECH A-12). Data were collected with the mask angle of 12°, where it is the optimum value of elevation mask angle [Yousef, 2004], epoch interval = 1 sec, where it is the optimum interval [Yousef and Ragheb, 2002] and occupation period > 1 hr. The coordinates of this point are shown in Table 1.

Table 1. The coordinates of fixed points C and R

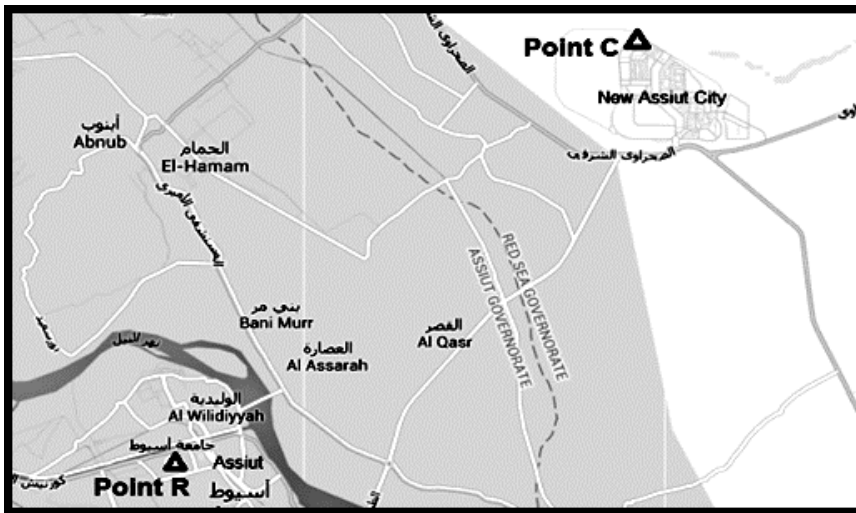| Coordinate frame	Point name			
ECEF frame X, Y and Z	Point C	4847990.25	2944869.44	2906897.90
	Point R	4857809.62	2938766.27	2896650.05
Geodetic frame (WGS 84) Lat, Long, h_{elip}	Point C	27º 17' 25.06754"N	31º16'34.40477"E	128.346
	Point R	27º 11'11.23584"N	31º 10'19.69518"E	90.848
Old Egypt 1906 E, N, h_{orth}	Point C	642190.7	509720.12	115.612

Fig. 2. The studied area

SINGLE DIFFERENCE PROCESS

Firstly, cycle slip count and place must be determined in taking sample in our observations to evaluate the performance of the studied methods in detecting it. The theoretical solution is to determine the ambiguity value, but this task isn't trivial. So the other way depends on removing this unknown ambiguity value by using the Single Difference (SD) in time between single receiver and single satellite at two constitute epochs (Fig. 3), where this technique removes the carrier

phase ambiguity term, because this ambiguity term is constant for the entire observation session [Bossler et al., 2002]. Also the SD technique reduces the ephemeris, ionospheric, and tropospheric errors, if epoch interval is short (less than 1min) [Ogaja, 2011].
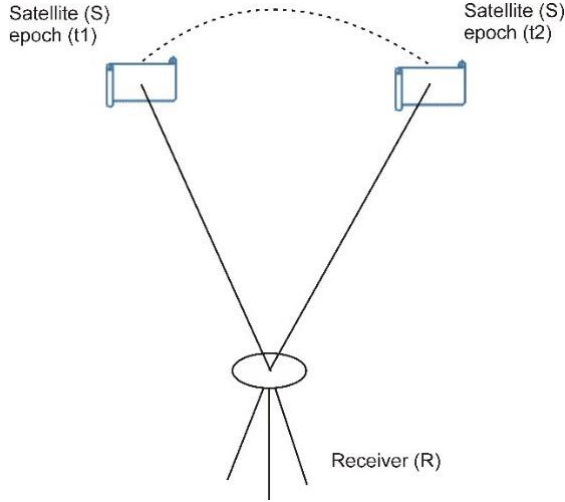

Fig. 3. Single Difference technique (one receiver observing one satellite at two epochs)

At single difference technique the givens data are the phase observations from one satellite (s) to one receiver (r) at two different epochs (t1 and t2) [Ogaja, 2011]. The difference between two consecutive epochs is as follows.

- Phase equation at epoch t1:

$$\emptyset_{L_i}^{t1} = \rho^{t1} + c[\delta t_r^{t1} - \delta t_s^{t1}] + T^{t1} - I^{t1} + ERt^{t1} + \lambda_{L_i} N_{L_i}{}^{t1} + Mpath^{t1} + \varepsilon_p^{t1} \ (1)$$

- Phase equation at epoch t2:

$$\emptyset_{L_i}^{t2} = \rho^{t2} + c[\delta t_r^{t2} - \delta t_s^{t2}] + T^{t2} - I^{t2} + ERt^{t2} + \lambda_{L_i} N_{L_i}{}^{t2} + Mpath^{t2} + \varepsilon_p^{t2} \ (2)$$

- The difference between (1) and (2) is as follows:

$$\Delta\emptyset_{L_i} = \Delta\rho - \Delta(c * \delta t_s) + \Delta T - \Delta I + \Delta ERt$$

Or $$\Delta\emptyset_{L_i} - \Delta\rho = \Delta(c * \delta t_s) + \Delta T - \Delta I + \Delta ERt \qquad (3)$$

where:

ϕ_{Li} — the measured phase of L_i (L_1 or L_2), cycle;

ρ — true geometric range, m;

c — speed of light, m/s;

δt_r — receiver clock error, sec;

δt_s — satellite clock error, sec;

T   — tropospheric delay, m;

I   — tropospheric delay, m;

ERt   — earth rotation error, m;

Δ — single difference operator;

Mpath — the multipath error, m; but, in this research, the observing must be done in an open area, so 'Mpath' error is approximately zero.

The equation (3) is a condition equation to identify if the observations have cycle slip error or not; and to test the precision of the proposed detected method in this research. But firstly the range of each error change between two constitutive epochs must be known, which are Δt_s, ΔT, ΔI, and ΔERt; that by estimating the values of these errors. The equations of these errors are listed below.

- The satellite error (t_s) can be estimated from the equation (4) [Ashby, 2003]:

$$t_s = af_0 + af_1(Tt_r - t_{oe}) + af_2(Tt_r - t_{oe})^2 + \Delta_{rel} \tag{4}$$

$$\Delta_{rel} = e\sqrt{a}\,(\sin E_k) \tag{5}$$

where:

af_0, af_1, af_2 — coefficients are available in the navigation message file;

Tt_r — transmission time;

toe   — ephemeris reference time;

Δ_{rel} — relativistic correction;

E   — eccentricity;

a   — orbital semi-major axis.

- The tropospheric error (T) can be predicted using Hopfield model (6) [Chaib et al., 2007]:

$$T = \frac{Kd}{sin(El^2 + 1.904 \times 10^{-3})^2} + \frac{Kw}{sin(El^2 + 0.6854 \times 10^{-3})^2} \tag{6}$$

$$Kd = 1.55208 \times 10^{-4} \times Pamb \times \frac{40136.0 + (148.72 * Tamb)}{Tamb + 273.16} \qquad (7)$$

$$Kw = -0.282 \times \frac{Pvap}{(Tamb + 273.16)} + 8307.2 \times \frac{Pvap}{(Tamb + 273.16)^2} \qquad (8)$$

where:

T_{amb} — ambient air temperature, Cel;

Pamb   — ambient air pressure, kpa;

Pvap   — ambient vapor pressure, kpa;

El   — the satellite vehicle's elevation in radian;

Kd and Kw   — are the dry an wet components respectively.

- The ionospheric error (I) can be predicted using the approximately form of Klobuchar's model (9) [Chaib et al., 2007; Klobuchar, 1987]:

$$I = t_{ion} = [1 + 16 \times (0.53 - EL)^3 \times 5 \times 10^{-9}] \qquad (9)$$

- The earth rotation error (ERt) can be estimated from the following equation (10) [19]:

$$ERt = \frac{\omega_E}{c}(X_{sat}Y_{rec} - Y_{sat}X_{rec}) \qquad (10)$$

where:

ω_E — earth turn rate $7.2921151467 \times 10^{-5}$, rad/sec;

X_{sat} and Y_{sat} — satellite horizontal coordinates, m;

X_{rec} and Y_{rec} — receiver horizontal coordinates, m.

   By applying the previous equations on our observations of satellite PRN 6, as an example, at 'Point C and Point R', taking sample size (360 epochs) with observation epoch interval 1 second, the values of t_s, T, I, and ERt can be determined. Then the values of change of each error per 1 sec (error difference), the average value and standard deviation value could be estimated (Table 2). The relations of these difference values for each error with time and its histogram are shown in Figure 4.

   From Figure 4 it was found that the resultant error differences from each estimated error have a normal distribution, so the maximum allowable value for each error is equal the mean value plus or minus three of the standard deviation value [www.3sigma]. Then the maximum value of the right part of (3) can be estimated and it would equals about 15.02 cm (approximately 1 cycle).

Table 2. The average value and standard deviation of each error change
Δt_s, ΔT, ΔI and ΔERt for 1 sec

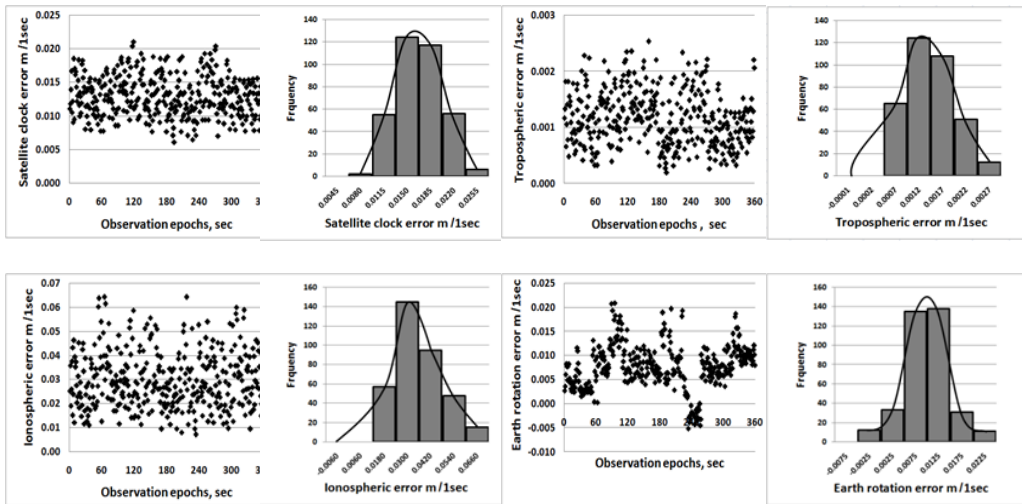| Points	Δt_s, m/sec		ΔT, m/sec		ΔI, m/sec		ΔERt, m/sec	
	μ	σ	μ	σ	μ	σ	μ	σ
Point C	0.015	0.0035	0.0012	0.0005	0.03	0.012	0.0075	0.005
Point R	0.012	0.005	0.0016	0.0003	0.05	0.016	0.006	0.004

Fig. 4. The relations between each error difference / 1sec in time and their histograms
'Taking Point C as example'

The cycle slip error, place and value, on our testing observations data can be detected easily by applying SD equation (3). Where the receiver coordinate is known and the precise geometric distance between the receiver and satellite can be estimated at any epoch by using the precise ephemeris navigation data. So if the value of the left part of (3) is higher than 1 cycle; then the cycle slip error is founded.

The following table shows the detected cycle slip error using Single difference technique at five observation minutes (interval 1 second), from the phase observations of satellite PRN 6, at point C and point R (Table 3).

Table 3. The detected count of cycle slip error in five minutes of observation data
(interval 1 second) at point C and point R

Point C				Point R		
Epoch	Error status	Cycle Slip Count		Epoch	Error Status	Cycle Slip Count
1–42	Yes	>100000		1–46	Yes	>100000
43–46	Yes	1500		47–48	Yes	2000
47–49	Yes	400		49–52	Yes	250
50–80	No	0		53–92	No	0
81–84	Yes	10		93–94	Yes	10
85–117	No	0		95–123	No	0
118–119	Yes	5		124–127	Yes	5
120–122	Yes	3		128–193	No	0
123–128	Yes	2		194–196	Yes	1
129–246	No	0		197–230	No	0
247–250	Yes	1		231–235	Yes	1
251–300	No	0		236–300	No	0

DETECTED METHODS

There are many methods for cycle slip detecting and predicting, but this research will focus on the well-established methods, which are Phase-Phase and Phase-Code method and comparing it with the most precise method, which is named Doppler measurements method. A short study on the Doppler method and its precision in detecting and predicting the cycle slip error in our data, will be presented in the following section.

Doppler Measurements Method

This technique takes the advantage of the fact that, the Doppler measurements are immune to cycle slips because they are computed values, where these Doppler measurements are equal to the expected change at carrier phase measurement from two adjacent epochs [Silva, 2013]. To clarify, when a cycle slip found

in a certain epoch, the Doppler measurement doesn't equal to the carrier phase time difference between this epoch and its previous epoch. The carrier phase variation between two adjacent epochs can be estimated by Doppler data according to the following equation (11) [Dai, 2012]:

$$[\emptyset_{Li}(t) - \emptyset_{Li}(t-1)] = [D_{Li}(t) + D_{Li}(t-1)] * dt/2 \qquad (11)$$

where:

D — Doppler frequency measurements, MHz;

dt — the sampling interval, sec.

So if this condition equation is not achieved; that means there is cycle slip error affects the phase observations. When this method was applied on our phase observations data it was found that this method succeed in detecting and predicting smallest cycle slip sizes (1 cycle), as shown in Table 4. The resultant precision of this method is agreed by many researchers [Dai, 2012], Ren et al., 2012] in case the local oscillator has low bias [Ren et al., 2011].

Table 4. The possibility of the usage methods for detecting cycle slip error

Cycle Slip Count Prediction method	> 100	10	5	1
Doppler method (the precise method)	Detected	Detected	Detected	Detected
Phase-Code	Detected	Detected	**Not Detected**	**Not Detected**
Phase-Phase	Detected	Detected	Detected	**Not Detected**
Modified Phase-Code	Detected	Detected	Detected	Detected
Modified Phase-Phase	Detected	Detected	Detected	Detected

Phase-Code Differencing Method

This method depends on the comparison between observables (phase and code), where the code measurements are immune to the cycle slip error. At stand-alone GPS receiver, the observations equations for pseudorange code and carrier phase measurements can be formulated as (12) and (13) [Dai, 2012]:

$$P_{L_i}^m(t) = \rho^m(t) + c[\,\delta t_r(t) - \delta t_s(t)] + T^m(t) + I^m(t) + ERt(t) + \\ + bias_p^m \tag{12}$$

$$\emptyset_{L_i}^m(t) = \rho^m(t) + c[\delta t_r(t) - \delta t_s(t)] + T^m(t) - I^m(t) + ERt(t) + \lambda_{L_i}N_{L_i} + \\ + \varepsilon_{L_i}^m \tag{13}$$

By using the differencing technique between two consecutive epochs, free of cycle slip, at time (ti and tj), to eliminate the most affecting errors on the phase and code measurements, the (12) and (13) can be written as:

$$\Delta P_{L_i}^m = \Delta\rho^m + c[\Delta\delta t_r - \Delta\delta t_s] + \Delta T^m + \Delta I^m + \Delta ERt + \Delta bias_p^m \tag{14}$$

$$\Delta\emptyset_{L_i}^m = \Delta\rho^m + c[\Delta\delta t_r - \Delta\delta t_s] + \Delta T^m - \Delta I^m + \Delta ERt + \lambda_{L_i}\Delta N_{L_i} + \Delta\varepsilon_p^m \tag{15}$$

When subtract (14) from (15) most of the errors are removed but the difference of ionospheric error doubled because its sign in phase equation reverse its sign in code equation. But the change in ionospheric delay between adjacent epochs would be very small so it can be neglected, this assumption is case of small sampling interval (less than 1 minute) [Dai, 2012; Kim, 2002]. Also, the time difference between ambiguities (N) is zero in case of no cycle slip [Ashby, 2003] thus, the equation resulted would be as follow (16):

$$\Delta P_{L_i}^m = \lambda_{L_i} * \left[\Delta\emptyset_{L_i}^m\right] \tag{16}$$

If this condition equation is not achieved; that means there is a cycle slip error affects the observations. When this method applied on our phase observations data it was found that; this method succeed in detecting and predicting cycle slip size $\geq$ 10 cycles, as shown in Table 4, because the code measurements have high noise level and the ionospheric change might have high variation [Ren et al., 2012; Karaim et al., 2014].

Phase-Phase Differencing Method

This method depends on the comparison between observables (phase 1 and phase 2), where the phase measurements have low noise effect. The observation equations for carrier phases measurements (L1 and L2) at the absolute positioning is (13) and can be formulated for each phase in (17) and (18) [Dai, 2012]:

$$\emptyset_{L_1}^m(t) = \rho^m(t) + c[\delta t_r(t) - \delta t_s(t)] + T^m(t) - I^m(t) + ERt(t) + \lambda_{L_1}N_{L_1} +$$
$$+ \varepsilon_{L_1}^m \tag{17}$$

$$\emptyset_{L_2}^m(t) = \rho^m(t) + c[\delta t_r(t) - \delta t_s(t)] + T^m(t) - \left(\frac{f_1}{f_2}\right)^2 I^m(t) + ERt(t) +$$
$$+ \lambda_{L_2}N_{L_2} + \varepsilon_{L_2}^m \tag{18}$$

where:

f_1 and f_2 — frequencies of phases L_1 and L_2 respectively, MHz.

By using the differencing technique between two consecutive epochs, free of cycle slip, at time (ti and tj), to eliminate the most affecting errors on the phases measurements, the (17) and (18) can be written as follows:

$$\Delta\emptyset_{L_1}^m = \Delta\rho^m + c[\Delta\delta t_r - \Delta\delta t_s] + \Delta T^m - \Delta I^m + \Delta ERt + \lambda_{L_1}\Delta N_{L_1} + \Delta\varepsilon_{L_1}^m \tag{19}$$

$$\Delta\emptyset_{L_2}^m = \Delta\rho^m + c[\Delta\delta t_r - \Delta\delta t_s] + \Delta T^m - \left(\frac{f_1}{f_2}\right)^2 \Delta I^m + \Delta ERt + \lambda_{L_2}\Delta N_{L_2} +$$
$$+ \Delta\varepsilon_{L_2}^m \tag{20}$$

The change in errors at (19) and (20) from epoch to adjacent epoch are very small, so it can be neglected. Also, this assumption is right at small sampling interval (less than 1 minute), and the time difference between ambiguities (N) is zero in case of no cycle slip [Ashby, 2003] thus, the equation resulted as follow (21):

$$\Delta\emptyset_{L_1}^m - \Delta\emptyset_{L_2}^m = 0 \tag{21}$$

When this method was applied to our phase observations data using this condition equation, it was found that this method succeed in detecting and predicting cycle slip size ≥ 5 cycles [Ren et al., 2012] as shown in Table 4. Because the ionospheric change might have high variation.

MODIFICATION FOR PHASE-CODE AND PHASE-PHASE METHODS

This modification aims to increase the precision of the Phase-Code and Phase-Phase methods in detecting small cycle-slips [Ren et al., 2012] by developing

a new algorithm to determine the change in the ionospheric values and code noise from epoch to epoch by solving all observables equations by least square technique. The linearized observations equations system can be represented using the matrix notation as follow (22) [Xu, 2007]:

$$AL + v = X \tag{22}$$

where:
X — Matrix of the unknowns;
A — Matrix of coefficients;
L — Matrix of the observation.

After subtracting each observable equation at certain epoch from the adjacent epoch, the final forms of all observables equations according to the form of basic equation of Least Square technique (22), are as follows:

$$\Delta\emptyset_{L_1}^m + v_1 = \Delta\rho^m - \Delta I^m \tag{23}$$

$$\Delta\emptyset_{L_2}^m + v_2 = \Delta\rho^m - \left(\frac{f_1}{f_2}\right)^2 \Delta I^m \tag{24}$$

$$\Delta P_{L_1}^m + v_3 = \Delta\rho^m + \Delta I^m + \Delta bias_{L_1}^m \tag{25}$$

$$\Delta P_{L_2}^m + v_4 = \Delta\rho^m + \left(\frac{f_1}{f_2}\right)^2 \Delta I^m + \Delta bias_{L_2}^m \tag{26}$$

The related least squares normal equation can be formed then as follow [Xu, 2007]:

$$X = (A^T A)^{-1} A^T L \tag{27}$$

Where the matrices of these equation terms can detailed as follows:

$$X = \begin{bmatrix} \Delta\rho^m \\ \Delta I^m \\ \Delta bias_{L_1}^m \\ \Delta bias_{L_2}^m \end{bmatrix} \quad A = \begin{bmatrix} 1 & -1 & 0 & 0 \\ 1 & -\left(\frac{f_1}{f_2}\right)^2 & 0 & 0 \\ 1 & 1 & 1 & 0 \\ 1 & \left(\frac{f_1}{f_2}\right)^2 & 0 & 1 \end{bmatrix} \quad L = \begin{bmatrix} \Delta\emptyset_{L_1}^m \\ \Delta\emptyset_{L_2}^m \\ \Delta P_{L_1}^m \\ \Delta P_{L_2}^m \end{bmatrix}$$

Solving this equation, the unknown value can be determined, which are $\Delta\rho^m$, ΔI^m, $\Delta bias_{L_1}^m$ and $\Delta bias_{L_2}^m$. These values can be used for enhancing the Phase-Phase and the Phase-Code methods, where the problems of ionospheric doubling and the code noise that affects the Phase-Code method and also the ionospheric high variation affects the Phase-Phase method can be solved.

When these methods were applied again to our observation data of point C and point R after the previous modifications, it was found that this method succeed in detecting and predicting cycle slip size equal to 1cycle, as shown in Table 4.

CONCLUSIONS

The algorithm developed in this research succeed in increasing the cycle slip error detecting precision for Phase-Code differencing method, and Phase-Phase Differencing Method. Their precision become close to, or equal, the precision of Doppler measurement method, where they can detect and predict the smallest cycle slips of size even of 1 cycle. The new algorithm succeed in determining the error of the aforementioned methods, which are ionospheric doubling and the code noise effects in the Phase-Code method and the high ionospheric variation effects in the Phase-Phase method.

REFERENCES

[1] Ashby N., Relativity in the Global Positioning System, Journal of Living Review in Relativity, 2003, Vol. 6.

[2] Banville S. et. al., Cycle-Slip Correction for Single-Frequency PPP, Proceedings of the Institute of Navigation ION GNSS, 2012.

[3] Bossler J. D. et. al., Manual of Geospatial Science and Technology, Taylor & Francis is an imprint of the Taylor & Francis Group, 2002.

[4] Cai C. et. al., Cycle Slip Detection and Repair for Undifferenced GPS Observations Under High Ionospheric Activity, Journal of GPS Solution, 2013, Vol. 17, pp. 247–260.

[5] Chaib C. et. al., Measurements for GPS Meteorological Applications, Journal of Energies Renouvelables, 2007, Vol. 10, No. 2, pp. 299–309.

[6] Dai Z., MATLAB Software for GPS Cycle-Slip Processing, Journal of GPS Solution, 2012, Vol. 16, pp. 267–272.

[7] Dawod G. M., Some Considerations in the Adjustment of GPS-Derived Baselines in the Network Mode, Master's thesis, Department of Geodetic Science and Surveying, Ohio State University, 1991.

[8] Gustavsson P., Development of a Matlab Based GPS Constellation Simulation for Navigation Algorithm Developments, Master's Thesis, Space Science Department, Lulea University of Technology, 2005.

[9] Karaim M. et. al., GPS Cycle Slip Detection and Correction at Measurement Level, British Journal of Applied Science & Technology, 2014, Vol. 29, No. 4, pp. 4239–4251.

[10] Kim D., Instantaneous Real-Time Cycle-Slip Correction For Quality Control of GPS Carrier-Phase Measurements, Proceedings of the Institute Of Navigation ION GNSS, 2002.

[11] Klobuchar J. A., Ionospheric Time-Delay Algorithm for Single-Frequency GPS Users, IEEE Transaction on Aerospace and Electronic Systems, 1987, Vol. 23, No. 3.

[12] Li X., M. Ge, Zhang H., Wickert J., A method for improving uncalibrated phase delay estimation and ambiguity-fixing in real-time precise point positioning. Journal of Geodesy, 2013, 87(5), pp. 405–416.

[13] Li X., Zhang X., Guo F., Predicting atmospheric delays for rapid ambiguity resolution in precise point positioning, Advances in Space Research, 2014, 54(5), pp. 840–850.

[14] Liu Z., A New Automated Cycle Slip Detection and Repair Method for a Single Dual-Frequency GPS Receiver, Journal of Geodesy, 2011, 85(3), pp 171–183.

[15] Ogaja C. A., Applied GPS for Engineers and Project Managers, American Society of Civil Engineers, 2011.

[16] Raju P. L. N., Fundamental of GPS, Satellite Remote Sensing and GIS Applications in Agricultural Meteorology, 2004, pp 121–150.

[17] Ren Z. et. al., Instantaneous Cycle-Slip Detection and Repair of GPS Data Based on Doppler Measurement, International Journal of Information and Electronics Engineering, 2012, Vol. 2, No. 2.

[18] Ren Z. et. al., A Real-time Cycle-slip Detection and Repair Method for Single Frequency GPS Receiver, Proceedings of 2nd International Conference on Networking and Information Technology, Singapor 2011.

[19] Seeber G., Satellite Geodesy, 2nd edition, Walter de Gruyter GmbH & Co. KG, 10785, Berlin 2003.

[20] Silva P., Cycle Slip Detection and Correction for Precise Point Positioning, Proceedings of the Institute of Navigation ION GNSS, 2013.

[21] Wu Y. et. al., Cycle Slip Detection Using Multi-Frequency GPS Carrier Phase Observations: A Simulation Study, Advances in Space Research, 2010, Vol. 46, pp. 144–149.

[22] Xu G., GPS Theory Algorithms and Applications, 2nd edition, Springer — Verlag, Berlin — Heidelberg 2007.

[23] Yousef M. A., Study the Effect of Elevation Mask on GPS Accuracy, Journal of Engineering Sciences, 2004, Vol. 32, No. 3, pp. 1281–1290.

[24] Zhang X., Li X., Instantaneous Re-initialization in Real-time Kinematic PPP with Cycle-slips Fixing, GPS Solutions, 2012, 16(3), pp. 315–327.

AHMED A. ELASHIRY
Beni-Suef University
eng_ahmedashiry@yahoo.com

MOHAMED A. YOUSSEF
Assiut University
aburakm@yahoo.com

MOHAMED A. ABDEL HAMID
Beni-Suef University
amonged@yahoo.com

STRESZCZENIE

Powszechnie znane są trzy metody wykrywania przeskoków fazowych (utraty cyklu, *cycle slip*) w fazowych pomiarach GPS. Są to: metoda Dopplerowska, metoda różnicy Faza-Kod i metoda różnicy pomiędzy fazami (Faza-Faza). Pierwsza z nich polega na porównaniu wartości obserwowanych i korzysta z faktu, że pomiary częstotliwości dopplerowskiej są odporne na przeskoki fazy. Metoda ta jest uważana za najbardziej dokładną spośród metod wykrywania utraty cyklu, albowiem pozwala wykrywać i przewidywać najmniejsze wartości utraty cyklu (1 cykl) pod warunkiem niewielkiego odstrojenia lokalnego generatora. Druga metoda polega na porównaniu wartości obserwowanych fazy i kodu z wykorzystaniem faktu, że pomiary kodowe są odporne na przeskoki cyklu. Jednakże metoda ta nie pozwala wykryć utraty cykli mniejszych niż dziesięć okresów z powodu wartości szumu pomiarów kodowych. Trzecia metoda polega na porównaniu wartości obserwowanych wyłącznie w domenie pomiarów fazowych w kolejnych epokach i uwzględnia fakt, że pomiary fazowe cechują się niższym zaszumieniem. Jednak ta metoda nie pozwala dostrzec przeskoków cyklu o wartości mniejszej niż 5 z powodu własności jonosfery.

Dla zwiększenia dokładności ostatnich dwóch metod i możliwości wykrycia pojedynczych przeskoków cyklu zaproponowano nowy algorytm wykrywania przeskoków fazy wywołanych zmianami stanu jonosfery pomiędzy epokami. Zostało to osiągnięte poprzez rozwiązywanie wszystkich równań obserwacyjnych metodą najmniejszych kwadratów. Ta modyfikacja pozwoliła wykrywać nawet pojedyncze przeskoki cyklu.